Lifescience Global

Journal of Coating Science and Technology
http://www.lifesciencesglobal.com/journals/journal-of-coating-science-and-technology

Simulation of Micro-Precoating Effect on Temperature Distribution in Plasma Thermal Spraying

Kelvii Wei Guo*

Department of Mechanical and Biomedical Engineering, City University of Hong Kong, 83 Tat Chee Avenue, Kowloon Tong, Kowloon, Hong Kong

Abstract: The effect of micro-precoating on temperature distribution of the plasma thermal spraying was simulated. After the plasma thermal spraying test with SS304 as precoating, the effect of micro-precoating on the wear loss and fatigue had been studied preliminarily. Results show that the surface temperature with micro-precoating is higher than that of without micro-precoating. Meanwhile, the heat affected zone with precoating is wider which effectively restrains the microcracks forming in the succedent coating. Subsequently, the wear and fatigue of the plasma thermal spray coating are significantly increased with the optimum micro-precoating thickness.

Received on 24-08-2017
Accepted on 30-10-2017
Published on 10-01-2018

Keywords: Simulation, Temperature distribution, Micro-precoating, Thermal spraying.

DOI: https://doi.org/10.6000/2369-3355.2017.04.03.1

1. INTRODUCTION

In recent years, micro technology has become one of the key disciplines, having a significant effect on the development of new products and production technologies, as well as on the introduction of new methods for medical treatment and diagnostics. Moreover, due to the enormous potential for new applications, in future, micro technology will increasingly affect our daily life with an impact, comparable to that of the industrial revolution in the 20th century, or the development of information technologies in the 21st century [1-4].

To date, a key issue associated with miniaturization is the tremendous increase in the heat dissipation per unit volume. Microstructures may enable engineered materials with unique thermal properties to allow significant enhancement or reduction of the heat flow rate [5-10]. Therefore, knowledge of thermal transport from the micrometer scale and thermal properties of microstructures is of critical importance to future technological growth. Also, the effect of micro-parts on the macrostructure, especially for the micro-precoating in the thermal spraying, has not been investigated in detail yet. Consequently, the complicated problems due to micro-precoating should be overcome. This research aims at investigating the effect of micro-precoating on the temperature distribution in the thermal spraying to overcome current problems in the thermal spray technology, especially for the microcracks.

2. EXPERIMENTAL MATERIAL AND PROCEDURES

The substrate was AISI 1045, and stainless steel 304 was used as precoating with 50 μm in thickness. The substrate was machined into 80 mm×60 mm×7.95~8 mm and carefully cleaned by acetone and pure ethyl alcohol to remove any contaminants on its surface. EIS-200ER plasma thermal spraying system made by Elionix, with accelerated voltage 2500 V, Ar gas flow rate 0.61 SCCM, current 16~20 mA and focus spot diameter of approximately 8 mm, was used to precoat the micro-stainless steel 304 film and irradiate the AISI 1045 steel. After irradiated, the surface morphology of precoating was observed by Scanning Electron Microscope (SEM) JEOL/JSM-5600, and the temperature was measured by apparatus attached with EIS-200ER.

3. COMPUTATIONAL MODEL

3.1. Equations for Temperature Distribution

Using energy balance, a differential equation can be obtained for the steady temperature distribution in a homogeneous isotopic medium, that is

$$\frac{\partial}{\partial x}\left(K_x \frac{\partial \theta}{\partial x}\right)+\frac{\partial}{\partial y}\left(K_y \frac{\partial \theta}{\partial y}\right)+\frac{\partial}{\partial z}\left(K_z \frac{\partial \theta}{\partial z}\right)=-q^B \quad (1)$$

*Department of Mechanical and Biomedical Engineering, City University of Hong Kong, 83 Tat Chee Avenue, Kowloon Tong, Kowloon, Hong Kong; Tel: 852-3442-4621; Fax: 852-3442-0172; E-mail: kelviiguo@yahoo.com

Where the boundary conditions are $\theta\big|_{s_1}=\theta_e$, $K_s\dfrac{\partial\theta}{\partial x}\Big|_{s_2}=q^s$.

For

$$\pi=\int_V\left\{K_x\left(\frac{\partial\theta}{\partial x}\right)^2+K_y\left(\frac{\partial\theta}{\partial y}\right)^2+K_z\left(\frac{\partial\theta}{\partial z}\right)^2\right\}d_V-\int_V\theta q^s d_V-\int_{s_2}\theta^s q^s d_s \tag{2}$$

After Eq. 2 is discrete for the element, and according to $\delta\pi=\sum_{e=1}^{n}\delta\pi_e=0$, it will be obtained

$$\overline{K^K}\overline{\theta}=\overline{\theta_s}+\overline{\theta_B}-\overline{C\theta}+\overline{K^c}(\theta_c-\overline{\theta^s})+\overline{K^r}(\theta_r-\overline{\theta^s}) \tag{3}$$

where *S*: isothermal boundary, *B*: the heat-input, *c*: the conductive and *r*: the irradiative.

3.2. Classical Size Effect on Thermal Conductivity Based on Geometric Considerations

In the ballistic transport limit when $\delta<\xi_b$ as shown in Figure **1**, if it is assumed that the mean free path in the film is the same as the micro-precoating thickness δ, i.e., $\xi_f=\delta$, then the conductivity ratio can be obtained as

$$\frac{\kappa_f}{\kappa_b}=\frac{\xi_f}{\xi_b}=\frac{1}{K_n} \tag{4}$$

where ξ_b is called the bulk mean free path, $K_n=\dfrac{\xi_b}{\delta}$ is the Knudsen number, adopted from the theory of rarefied gas dynamics, for electrons or phonons. In the intermediate region, the Matthiessen's rule can be applied

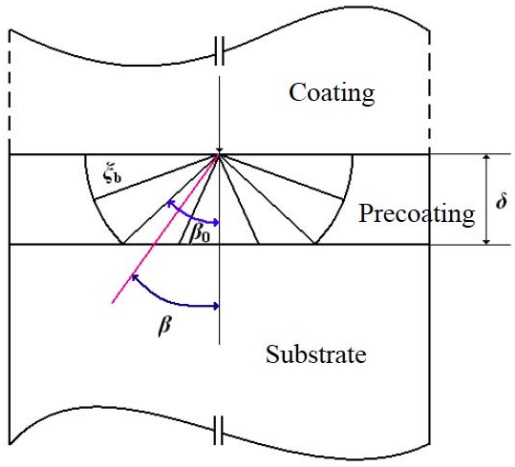

Figure 1: Free path reduction due to boundary scattering originated form the micro-precoating surface.

$$\frac{1}{\xi_{eff}}=\frac{1}{\xi_b}+\frac{1}{\xi_f} \tag{5}$$

Accordingly

$$\frac{\kappa_{eff}}{\kappa_b}=\frac{\xi_{eff}}{\xi_b}=\frac{1}{1+K_n} \tag{6}$$

However, the distribution of free path is not taken into consideration for simplicity in the above equations. In other words, all paths are assumed to be the same as the mean free path in the bulk. When $\delta>\xi_b$, it may be assumed that all energy carriers originate from the boundary. From Figure **1**, it is obtained

$$\xi(\beta)=\begin{cases}\delta/\cos\beta, 0<\beta<\beta_0\\ \xi_b, \beta_0<\beta<\pi/2\end{cases} \tag{7}$$

The free paths should be averaged over the hemisphere, and the weighted average can be written and evaluated as follows:

$$\frac{\xi_f}{\xi_b}=\frac{\int_0^{2\pi}\int_0^{\pi/2}\xi(\beta)\sin\beta d\beta d\phi}{\int_0^{2\pi}\int_0^{\pi/2}\xi_b\sin\beta d\beta d\phi}=\frac{\ln(K_n)+1}{K_n} \tag{8}$$

Applying Matthiessen's rule, it is obtained

$$\frac{\kappa_{eff}}{\kappa_b}=\frac{\xi_{eff}}{\xi_b}=\left(1+\frac{K_n}{\ln K_n+1}\right)^{-1} \tag{9}$$

This equation, however, cannot be applied for small values of K_n since ln(K_n) becomes negative. Assumed Eq. is applicable for $K_n>5$. When $K_n<1$, it may be used

$$\frac{\kappa_{eff}}{\kappa_b}=\frac{\xi_{eff}}{\xi_b}=\left(1+\frac{K_n}{m}\right)^{-1} \tag{10}$$

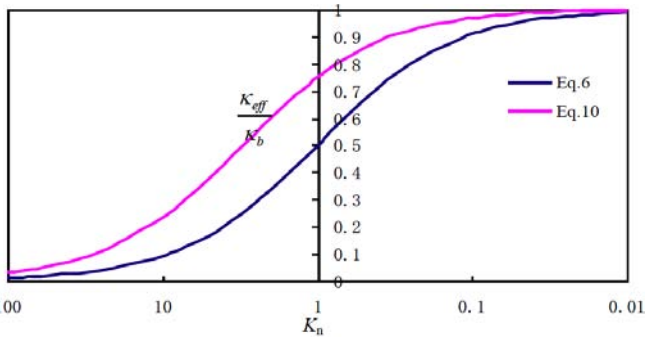

Figure 2: Reduction in thermal conductivity due to boundary scattering.

Where $m\approx3$ for thin films. Eq. 6 can be considered as a special case of Eq. 10 with $m=1$. In this research, the direction of transport and the anisotropic feature due to size effect are not considered due to spraying size.

The results calculated are plotted in Figure **2** to illustrate the size dependence of the effective thermal conductivity.

3.3. Hypothesis and Mesh

Based on the situations during the plasma thermal spraying and mainly focused on the effect of precoating, it is supposed that the spraying particles are considered as a Gaussian heat source with 8 mm in diameter to simplify the effect of high temperature spray particles on the micro-precoating. Meanwhile, the sample size is 80 mm (*x*) × 60 mm (*y*) ×

7.95~8 mm (*z*), its finite element (FE) mesh is shown in Figure **3**.

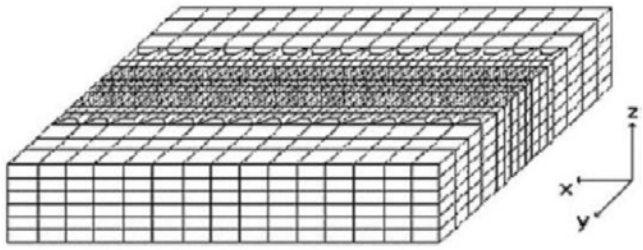

Figure 3: FE mesh for 3D numerical analysis.

4. RESULTS AND DISCUSSION

4.1. Temperature Distribution

The simulation results are shown in Figure **4**. It shows that the temperature with the precoating is higher than that of without precoating. Meanwhile, the heat affected zone increases correspondingly which can be observed more obviously in Figures **4e**, **f**. As a result, the heat input into the substrate will increase in the wider area to effectively restrain the cracks forming in the succedent plasma thermal spraying. The measured temperature results are shown in Figure **5**. It shows that the measured results match well with the simulated results.

Moreover, with the heat effect of the plasma spraying, the micro-precoating will be melted firstly, then under the effect of surface tension in nanoscale, it will be separated and formed numerous nanoparitcles as shown in Figure **6**. Therefore, the conductivity related to Eq. 6 and Eq. 10 should be revised. Consequently, the effect of micro-precoating will become more complicated which is neglected in this paper. In addition, if the precoating thickness is too thin, it will not have any distinct effect on the succedent plasma thermal spraying. When the precoating is too thick, the succedent coating will be cracked and peeled off resulted in failure coating. Therefore, the effect of precoating thickness on the temperature distribution is not listed here.

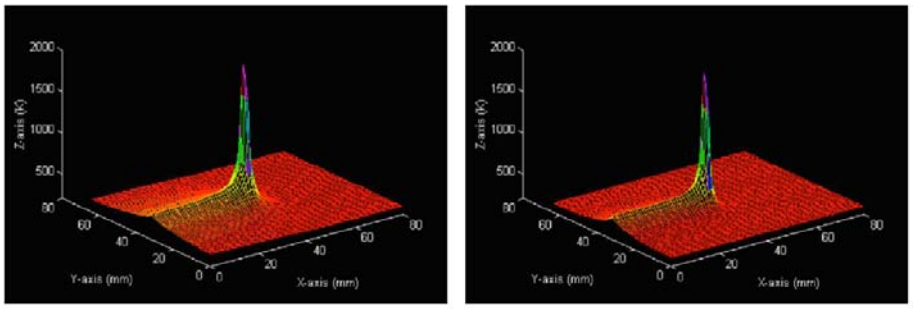

(i) With micro-precoating (ii) Without micro-precoating

(a) Temperature distribution on the 1st layer (z=50 μm)

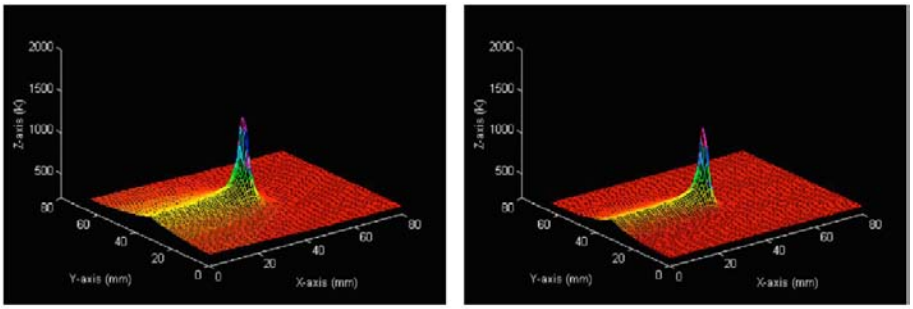

(i) With micro-precoating (ii) Without micro-precoating

(b) Temperature distribution on the 2nd layer (z=950 μm)

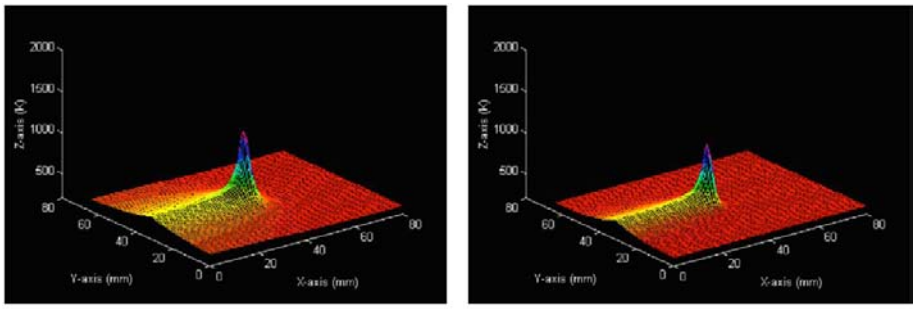

(i) With micro-precoating (ii) Without micro-precoating

(c) Temperature distribution on the 3rd layer (z=1950 μm)

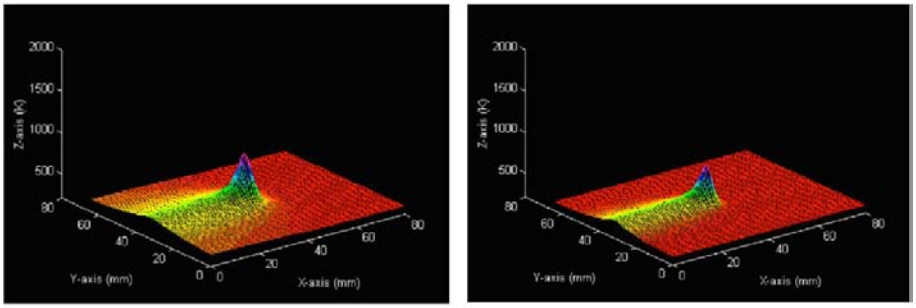

(i) With micro-precoating (ii) Without micro-precoating

(d) Temperature distribution on the 4th layer (z=3950 μm)

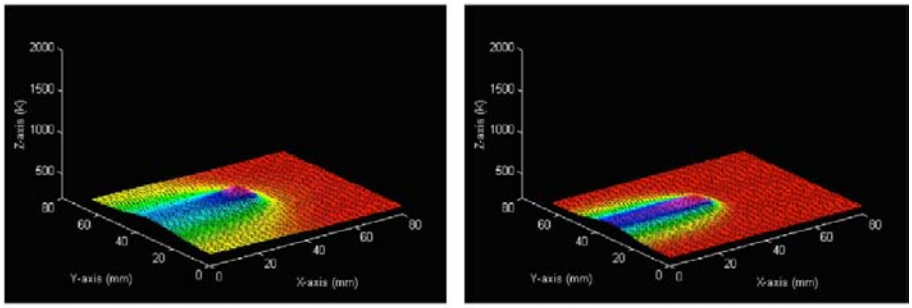

(i) With micro-precoating (ii) Without micro-precoating

(e) Temperature distribution on the 5th layer (z=5950 μm)

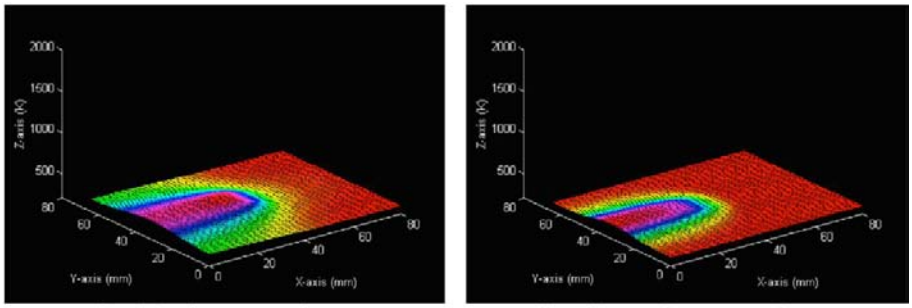

(i) With micro-precoating (ii) Without micro-precoating

(f) Temperature distribution on the 6th layer (z=7950 μm)

Figure 4: Temperature distribution of with/without precoating.

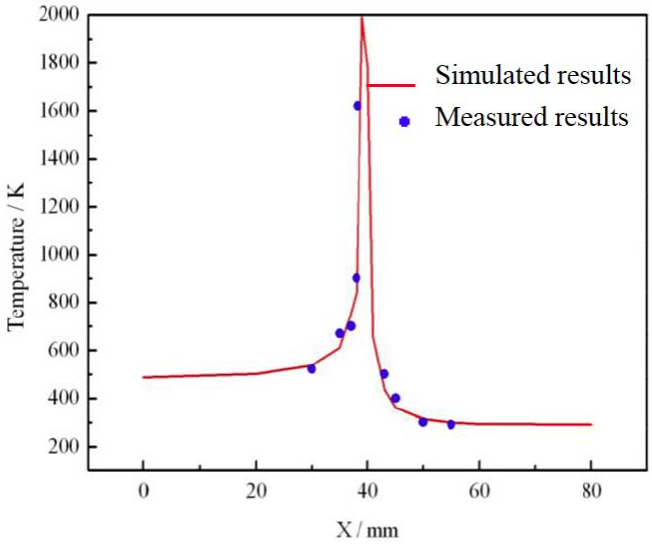

Figure 5: Surface temperature distribution in the processing center.

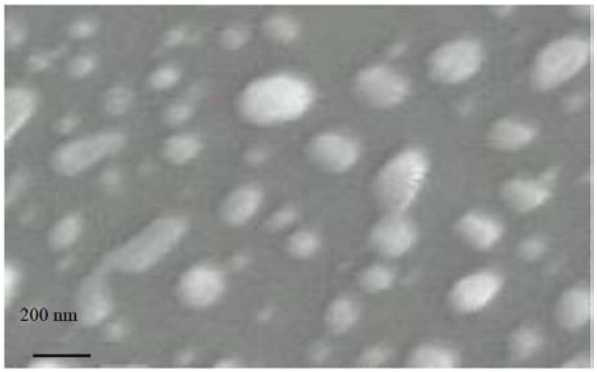

Figure 6: Nanoparticles forming in the initial micro-precoating.

4.2. Practical Application with Micro-Precoating

4.2.1. Wear Test

Wear was studied using a Cameron-Plint TE67 wear test rig (Made in UK) under dry conditions with a sliding speed 1.34

Table 1: Wear Loss under the Various Sliding Distances

Sample	Load (N)	Sliding distance (mm)	Lost weight (g)
A	36.7135	400	0.0010
		600	0.0013
		1600	0.0019
B	36.7135	400	0.0008
		600	0.0011
		1600	0.0015
C	36.7135	400	0.0006
		600	0.0008
		1600	0.0011
D	36.7135	400	0.0007
		600	0.0009
		1600	0.0014
E	36.7135	400	0.0010
		600	0.0015
		1600	0.0021

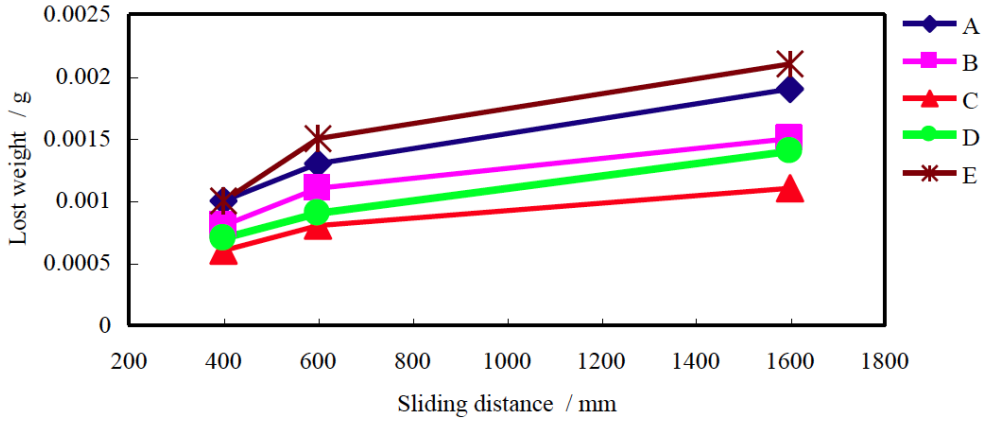

Figure 7: Relationship between the wear loss and sliding distance.

Table 2: Thickness of Precoating on the Substrates

Sample	A	B	C	D	E
Precoating	Non	Non	50 μm	60 μm	100 μm

m/s at constant applied loading of 36.7135 N. The stroke was set to 400, 600, 1600 mm, respectively.

Ultrasonic cleaner with 28–34 Hz frequency was used for cleaning samples. All well coated samples are ultrasonically cleaned in an acetone bath for 2 min, and carefully dried before/after wear testing. The weight of samples is measured by the Sartorius electronic weight before and after the wear testing with a minimum accuracy of 0.0001 g. The results are listed in Table **1** and plotted in Figure **7**. The corresponding precoating parameters are expressed in Table **2**. Generally speaking, the wear loss with precoating is lower than that without precoating. However, when the thickness of precoating exceeds 50 μm, the wear loss will be increased further, especially for the thicker thickness as shown in Figure **7** line E resulted in the lower quality coating.

4.2.2. Fatigue Test

The fatigue test was also carried on the Cameron-Plint TE67 wear test rig, where the maximum heating temperature is 800 °C with 2 min preservation, and the heating speed is 20 °C/min. Subsequently, samples are put into the 25 °C water. After cooling, samples are cleaned by acetone and alcohol, and dried by the drier. Finally, samples are observed by optical microscopy. The results are listed in Table **3**. It shows that with the precoating the fatigue properties of spray coating are increased to some extent, especially for the

Table 3: Fatigue Results with Various Conditions

Sample	Cycles (1 unit = 200 cycles)																	
	1	2	3	4	5	6	…	14	15	16	17	18	19	20	21	22	23	24
A	+	+	+	+	+	+	…	+	+	+	+	+	+	+	+	-		
B	+	+	+	+	+	+	…	+	+	+	+	+	+	+	+	+	-	
C	+	+	+	+	+	+	…	+	+	+	+	+	+	+	+	+	+	-
D	+	+	+	+	+	+	…	+	+	+	+	+	+	+	+	+	-	
E	+	+	+	+	+	+	…	+	+	+	+	-						

coating with 50 μm precoating. But, for spray coating with 100 μm precoating, the quality is decreased similar to that of wear test listed in Table **1**.

CONCLUSION

Simulation of the micro-precoating effect on the temperature distribution during the plasma thermal spraying was investigated. It shows that the surface temperature with micro-precoating is higher than that of without micro-precoating. Meanwhile, the heat affected zone with precoating is wider resulted in restraining the microcracks forming effectively in the succedent thermal spraying. Furthermore, the wear and fatigue of thermal spray coating are significantly increased with the optimum micro-precoating thickness.

REFERENCES

[1] Madou MJ. Microfabrication challenge. Analytical and Bioanalytical Chemistry 2004; 378: 11-14. https://doi.org/10.1007/s00216-003-2360-9

[2] Mark JJ. Microfabrication and nanomanufacturing. Boca Raton FL CRC/Taylor & Francis 2006.

[3] Christophe G. Microsystems engineering: metrology and inspection III. SPIE 2003.

[4] Fecht HJ, Werner M. The nano-micro interface: bridging the micro and nano worlds. Weinheim Wiley-VCH 2004.

[5] Jacobs PWM. Thermodynamics. London, UK: Imperial College Press 2013.

[6] Benenti G, Casati G, Saito K, Whitney RS. Fundamental aspects of steady-state conversion of heat to work at the nanoscale. Physics Reports 2017; 694: 1-124. https://doi.org/10.1016/j.physrep.2017.05.008

[7] Tyea RP, Maesono A. Characterization and thermal properties evaluation of thin films, wafers and substrates. Thermochimica Acta 1993; 218: 155-172. https://doi.org/10.1016/0040-6031(93)80419-B

[8] Stewart D, Norris PM. Size effect on the thermal conductivity of thin metallic wires: Microscale implications. Microscale Thermophysical Engineering 2000; 4: 89-101. https://doi.org/10.1080/108939500404007

[9] Kumar S, Vradis GC. Thermal conductivity of thin metallic films. Journal of Heat Transfer 1994; 116: 28-34. https://doi.org/10.1115/1.2910879

[10] Wight NM, Acosta E, Vijayaraghavan RK, McNally PJ, Smirnov V, Bennett NS. A universal method for thermal conductivity measurements on micro-/nano-films with and without substrates using micro-Raman spectroscopy. Thermal Science and Engineering Progress 2017; 3: 95-101. https://doi.org/10.1016/j.tsep.2017.06.009